J|A|C|S
ARTICLES
Published on Web 10/17/2002

Quinoxaline-Bridged Porphyrinoids

Jonathan L. Sessler,*,† Hiromitsu Maeda,†,‡,§ Toshihisa Mizuno,†
Vincent M. Lynch,† and Hiroyuki Furuta*,‡,§

Contribution from the Department of Chemistry and Biochemistry and Institute for Cellular and Molecular Biology, University of Texas at Austin, Austin, Texas 78712-1167 and Department of Chemistry, Graduate School of Science, Kyoto University, Kyoto 606-8502, Japan

Received June 19, 2002

Abstract: Quinoxaline-bridged porphyrinoids (**3**), the first macrocycles containing dipyrrolylquinoxaline (DPQ, **1**) subunits, were synthesized from the condensation of the diformyl-substituted DPQ derivatives (**2**) and 1,8-diaminoanthracene. The resulting structures were confirmed by X-ray analyses, which showed encapsulation of $CHCl_3$ molecules within the columnar channels established by the stacked arrangement of the individual macrocycles. The solution phase interactions with fluoride and dihydrogenphosphate anions were studied in the case of the unsubstituted system **3a** in CH_2Cl_2. The binding affinities for these anions, studied at the tetrabutylammonium salts, were found to be enhanced relative to those of the simple, unsubstituted monomeric DPQ "parent" system (**1a**), presumably as the result of the combined effects of preorganization and cooperative binding permitted by the pyrrole NH donor groups. Positive homotropic allosteric anion binding was observed and is ascribed to the structurally coupled nature of the two binding cavities present in the macrocycles. Support for this latter contention came from energy minimization studies.

Introduction

Molecules containing large lacunae have attracted considerable attention in recent years in part because of their ability to act as novel receptors for various encapsulated substrates and reaction precursors.[1] Among the various systems containing internal voids, expanded porphyrins, large oligopyrrolic macrocycles, are of particular interest because of the diversity of cation coordination and anion binding modes that they can conceivably support.[2] To date, most expanded porphyrins, including the recently reported "giant" systems of Setsune et al.,[3] have been derived from pyrroles and various sp^2 or sp^3 hybridized bridging carbon or nitrogen atoms. However, the introduction of other bridging elements, including ones that contain a built-in optical signaling functionality, could allow this approach to large molecule construction to be further generalized. Recently we reported that dipyrrolylquinoxaline (DPQ, **1a**; Scheme 1), a compound first synthesized by Oddo[4a] and later refined by Behr,[4b] can act as a useful anion receptor[5] in analogy to what is seen in the case of protonated sapphyrin,[6] neutral calixpyrrole,[7] and several other pyrrole-containing entities.[8] Unlike the cases of these previous systems, however, the binding of an anion, in particular fluoride, to DPQ triggers a change in color that is detectable by the naked eye. Thus, we reasoned that incorporating this fragment into a larger "expanded" macrocyclic framework might lead to novel porphyrinoids that could act as potential "molecular cages" for anionic, cationic, or neutral substrates. In accord with such thinking, we report here the synthesis, structure, and properties of the first quinoxaline-bridged porphyrinoids (compounds **3a**−**c**; Scheme 1). These systems represent a new type of expanded porphyrin analogue that, relative to **1**, acts as highly efficient fluoride and phosphate anion receptors in organic solution. They were also found to encapsulate neutral solvent species in the solid state.

Results and Discussion

Syntheses and Initial Characterization. As illustrated in Scheme 1, the quinoxaline-bridged porphyrinoids (**3a**−**c**) were

* To whom correspondence should be addressed. E-mail: sessler@mail.utexas.edu; hfuruta@cstf.kyushu-u.ac.jp.
† University of Texas.
‡ Kyoto University.
§ Present address: Department of Applied Chemistry, Graduate School of Engineering, Kyushu University, Fukuoka 812-8581, Japan.

(1) Dietrich, B.; Hosseini, M. W. In *Supramolecular Chemistry of Anions*; Bianchi, A., Bowman-James, K., Gracía-España, E., Eds.; Wiley-VCH: New York, 1997; pp 45−62.
(2) (a) Sessler, J. L.; Weghorn, S. J. *Expanded, Contracted and Isomeric Porphyrins*; Elsevier: New York, 1997. (b) Jasat, A.; Dolphin, D. *Chem. Rev.* **1997**, *97*, 2267−2340.
(3) (a) Setsune, J.-i.; Katakami, Y.; Iizuna, N.; *J. Am. Chem. Soc.* **1999**, *121*, 8957−8958. (b) Setsune, J.-i.; Maeda, S. *J. Am. Chem. Soc.* **2000**, *122*, 12405−12406.
(4) (a) Oddo, B. *Gazz. Chim. Ital.* **1911**, *41*, 248. (b) Behr, D.; Brandänge, S.; Lindström, B. *Acta Chem. Scand.* **1973**, *27*, 2411−2414.
(5) (a) Black, C. B.; Andrioletti, B.; Try, A. C.; Ruiperez, C.; Sessler, J. L. *J. Am. Chem. Soc.* **1999**, *121*, 10438−10439. (b) Anzenbacher, P., Jr.; Try, A. C.; Miyaji, H.; Jursíková, K.; Lynch, V. M.; Marquez, M.; Sessler, J. L. *J. Am. Chem. Soc.* **2000**, *122*, 10268−10272. (c) Mizuno, T.; Eller, L.; Wei, W.-H.; Sessler, J. L. *J. Am. Chem. Soc.* **2002**, *124*, 1134−1135. (d) Anzenbacher, P., Jr.; Tyson, D. S.; Jursíková, K.; Castellano, F. N. *J. Am. Chem. Soc.* **2002**, *124*, 6232−6233. (e) Sessler, J. L.; Maeda, H.; Mizuno, T.; Lynch, V. M.; Furuta, H. *Chem. Commun.* **2002**, 862−863.
(6) (a) Shionoya, M.; Furuta, H.; Lynch, V.; Harriman, A.; Sessler, J. L. *J. Am. Chem. Soc.* **1992**, *114*, 5714−5722. (b) Sessler, J. L.; Andrievski, A.; Genge, J. W. In *Advances in Supramolecular Chemistry*; Lehn, J. M., Ed.; JAI Press Inc.: Greenwich, CT, 1997; Vol. 4, pp 97−142. (c) Sessler, J. L.; Davis, J. M. *Acc. Chem. Res.* **2001**, *34*, 989−997.
(7) (a) Gale, P. A.; Sessler, J. L.; Král, V. K.; Lynch, V. M. *J. Am. Chem. Soc.* **1996**, *118*, 5140−5141. (b) Gale, P. A.; Sessler, J. L.; Allen, W. E.; Tvermoes, N. A.; Lynch, V. *Chem. Commun.* **1997**, 665−666. (c) Gale, P. A.; Sessler, J. L.; Král, V. *Chem. Commun.* **1998**, 1−8.
(8) (a) Coles, S. J.; Gale, P. A. *CrystEngChem* **2001**, *53*, 1−3. (b) Scherer, M.; Sessler, J. L.; Gebauer, A.; Lynch, V. *Chem. Commun.* **1998**, 85−86. (c) Bucher, C.; Zimmerman, R. S.; Lynch, V.; Král, V.; Sessler, J. L. *J. Am. Chem. Soc.* **2001**, *123*, 2099−2100. (d) Furuta, H.; Maeda, H.; Osuka, A. *J. Am. Chem. Soc.* **2001**, *123*, 6435−6436. (e) Takeuchi, M.; Shioya, T.; Swager, T. *Angew. Chem., Int. Ed.* **2001**, *40*, 3772−3776.

10.1021/ja0273750 CCC: $22.00

Scheme 1. Synthesis of Quinoxaline-Bridged Macrocycles **3a**−**c**

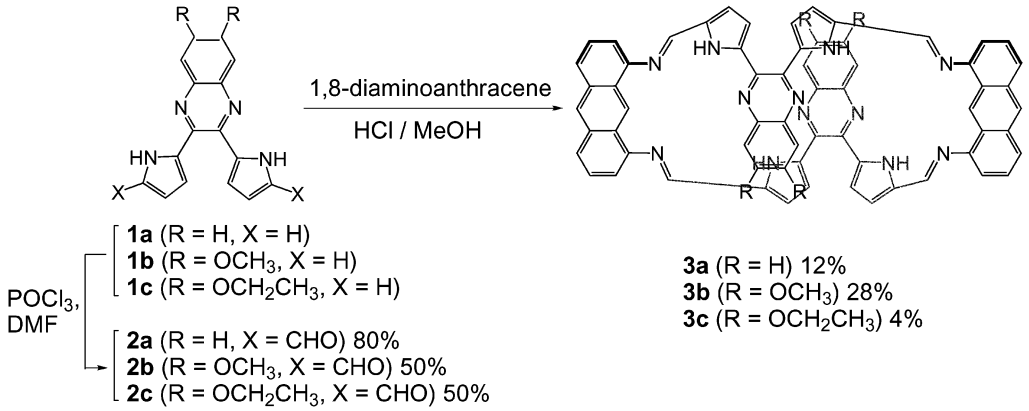

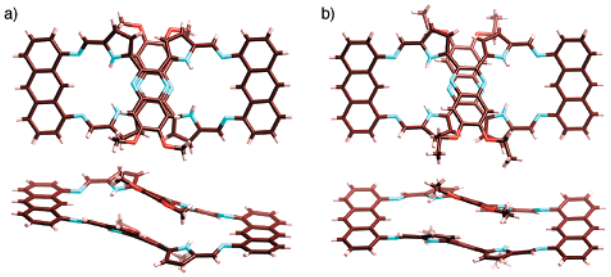

Figure 1. X-ray single-crystal structures of (a) **3b**·6$CHCl_3$·C_7H_8 and (b) **3c**·6$CHCl_3$, top view (top) and side view (bottom), respectively. Atom color code: brown, blue, red, and pink refer to carbon, nitrogen, oxygen, and hydrogen, respectively. Solvent molecules present within the macrocyclic cavity (see Figure 2) have been omitted for clarity.

prepared from the acid-catalyzed condensation of 1,8-diaminoanthracene[9] with a diformyl-substituted DPQ (**2a**−**c**). The latter intermediates were readily obtained from the DPQ derivatives **1a**−**c**[5a] by subjecting them to Vilsmeier formylation. The orange-colored Schiff-base products (**3a**−**c**) obtained in this way proved stable to air and moisture, allowing their structures to be assigned by ^{1}H NMR spectroscopy and high-resolution CIMS analysis. Trace quantities of other condensation products, including linear oligomers and higher order [3+3] macrocycles, were observed by CIMS spectra but could not be isolated in usable quantities. When hydrazine was used instead of 1,8-anthracenediamine in the condensation reaction of Scheme 1, ^{1}H NMR spectroscopic analysis and CIMS studies indicated the formation of a [2+2] diaza-bridged macrocyclic product. On the other hand, when 1,2-diaminobenzene was used, such analyses indicated the formation of a benzimidazole derivative of **2**. Unfortunately, in neither case could the inferred products be isolated in pure form because of their poor solubility.

Structural and Solid-State Supramolecular Effects. Clear evidence for the formation of the proposed macrocyclic products **3** came from X-ray diffraction analyses of **3b** (two structures)[10] and **3c** (Figure 1). Consistent with the proposed [2+2] motif, the structures reveal alternating pairs of DPQ and anthracene subunits linked by imino bridges. In all three structures, the two quinoxaline subunits point toward one another and appear

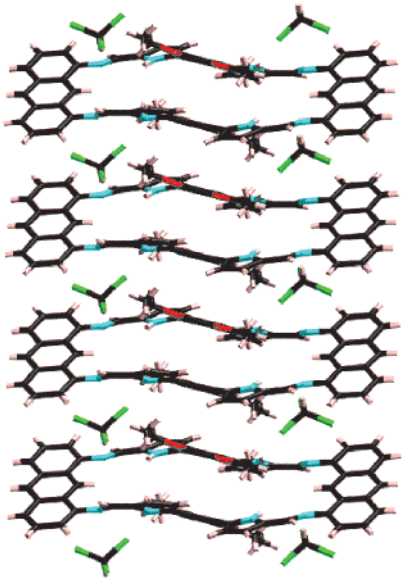

Figure 2. Side view of the $CHCl_3$-containing "molecular tube" present in crystalline samples of **3c**·6$CHCl_3$. Solvent molecules lying outside of the cavities have been omitted for clarity.

to be π-stacked "head-to-tail" with the distances between the two planes of **3b** and **3c** being 3.344(5)−3.552(7) and 3.506(11) Å, respectively. Further support for the contention that the structures of **3b** and **3c**, although quite similar in terms or their basic features, do differ somewhat is the observation that, in contrast to the case of **3b** (both structures), intermolecular stacking was observed in the case of **3c**. Here, a columnar structure containing a "molecular tube" motif is observed in the solid state (Figure 2).[11] Within this arrangement, the individual molecular subunits are separated by a distance of 3.539(13) Å at the point of closest approach. In the case of both **3b** and **3c**, the individual macrocycles are oriented so as to define a large internal cleft comprised of two similarly sized cavities. Six nitrogen atoms in total, that is, two pyrrole-NH, two imino-N, and two quinoxaline-N groups, point toward the inside of each of the cavities. In the structure shown in Figure 2, six $CHCl_3$ molecules per macrocycle **3c** are included within

(9) (a) Sessler, J. L.; Mody, T. D.; Ford, D. A.; Lynch, V. *Angew. Chem., Int. Ed. Engl.* **1992**, *31*, 452−455. (b) Meyer, S.; Andrioletti, B.; Sessler, J. L.; Lynch, V. *J. Org. Chem.* **1998**, *63*, 6752−6757. (c) Meyer, S.; Hoehner, M. C.; Lynch, V.; Sessler, J. L. *J. Porphyrins Phthalocyanines* **1999**, *3*, 148−158.

(10) The two structures of **3b** differ in the amount of solvent contained in the lattice but were otherwise quite similar, particularly in terms of the details of the macrocycle and its spatial arrangement.

(11) For molecular tubes based on π-stacking, see: (a) Laughlan, G.; Murchie, A. I. H.; Norman, D. G.; Moore, M. H.; Moody, P. C. E.; Lilley, D. M. J.; Luisi, B. *Science* **1994**, *265*, 520−524. (b) Ranganathan, D.; Haridas, V.; Gilardi, R.; Karle, I. L. *J. Am. Chem. Soc.* **1998**, *120*, 10793−10800. (c) Forman, S. L.; Fettinger, J. C.; Pieraccini, S.; Gottarelli, G.; Davis, J. T. *J. Am. Chem. Soc.* **2000**, *122*, 4060−4067. (d) Shi, X.; Fettinger, J. C.; Davis, J. T. *J. Am. Chem. Soc.* **2001**, *123*, 6738−6739. (e) Matile, S. *Chem. Soc. Rev.* **2001**, *30*, 158−167.

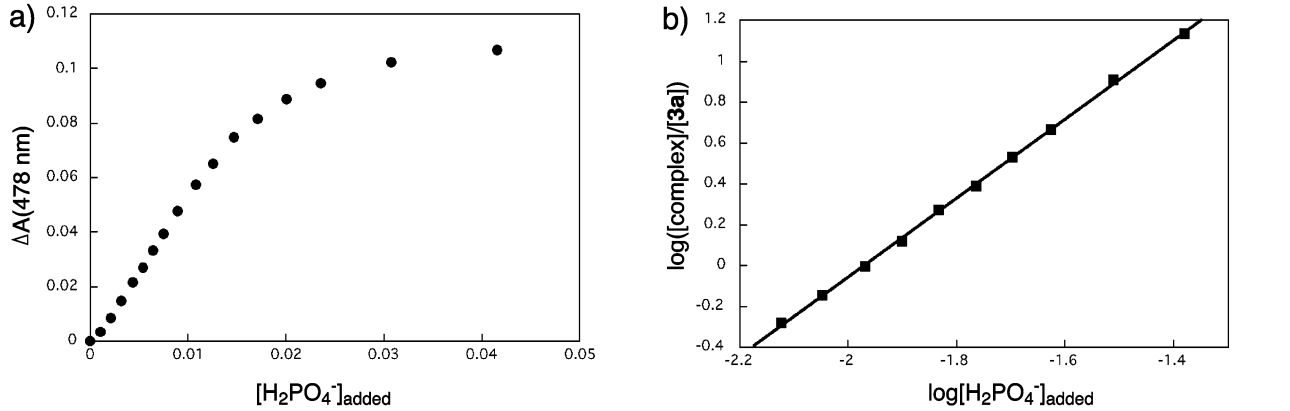

Figure 3. (a) Titration plots (observed binding profiles) and (b) corresponding linear Hill plots associated with the interactions between **3a** (1.2×10^{-5} M) and $H_2PO_4^-$ (studied as its tetrabutylammonium (TBA) salt in CH_2Cl_2).

the cleft, held there via hydrogen-bonding interactions involving the chloroform CH protons and the quinoxaline and/or Schiff-base imine nitrogens, as well as the alkoxy oxygens. Similar binding interactions are seen in the two structures of **3b**.[12] Thus, the "molecular tube" defined by **3c** in the solid state derives not only from quinoxaline subunit π-stacking but also from hydrogen-bonding networks involving the $CHCl_3$ molecules encapsulated within the channels. In other words, the cavities of the quinoxaline-containing macrocycles behave as hydrogen-bonding donating and accepting sites in the solid state.

As they contain a 1,8-disubstituted anthracene cross-conjugated "gap" within their overall π-electron frameworks, systems **3a**−**c** are expected to be nonaromatic. The ^{1}H NMR spectrum ($CDCl_3$) of **3b**, chosen for study because of its relatively high solubility, is consistent with such an expectation. For instance, two signals ascribable to the β-pyrrolic protons were observed at 6.61 and 6.51 ppm, respectively. Also, a resonance due to the inner NH proton was seen at 10.87 ppm, a chemical shift that is consistent with both the proposed nonaromatic formulation and the existence of hydrogen-bonding interactions involving the pyrrolic-NH and the imino-N or quinoxaline-N atoms. By contrast, the quinoxaline-H signal of **3b** was observed at relatively high field as compared to that of **2b** (6.92 vs 7.28 ppm). Such an upfield shift is consistent with the π-stacking seen in the solid state.

Anion Binding Properties. While considerably less soluble than **3b** and **3c**, macrocycle **3a** bears the closest analogy to **1a**, the DPQ system studied previously.[5a] Accordingly, its anion binding properties were investigated using standard UV−vis methods. The absorption spectrum of **3a** recorded in CH_2Cl_2 is characterized by two broad bands at 367 and 427 nm. Upon the addition of increasing quantities of tetrabutylammonium fluoride (TBAF), new bands at 329 and 480 nm were seen to grow in at the expense of those originally present, with good isosbestic behavior being seen.[13] The titration curve for the binding between **3a** and fluoride (F^-) in CH_2Cl_2 was consistent with an allosteric effect. The association constant, log*K*, and the coefficient obtained when the data were fit to the Hill equation were calculated as 11.0 and 2.2, respectively. Similar spectral behavior was observed when **3a** was titrated with the TBA salt of $H_2PO_4^-$ in CH_2Cl_2, a finding that is consistent with the binding mode of $H_2PO_4^-$ being similar to that of F^- (Figure 3). Here, the association constant, log*K*, and Hill coefficient were found to be 3.8 and 1.9, respectively. These findings lead to the suggestion that once a single F^- or $H_2PO_4^-$ is bound in the cavity of **3a**, the subsequent capture of a second anion is facile. To the extent this is true, direct quantitative comparisons with **1a** are not possible. However, it is noteworthy that the values of $\sqrt{K}$, corresponding to hypothetical 1:1 bindings between **3a** and F^- and $H_2PO_4^-$ (3×10^5 and 80 M^{-1}, respectively), are higher than the comparable 1:1 K_a values for **1a** in the same solvent (1.82×10^4 and 60 M^{-1}).[5a,14−16]

Support for these experimentally based conclusions comes from geometry optimization studies. Ab initio calculations, carried out at the HF/3-21G level, for structure **3a** and its various putative fluoride anion complexes were used to evaluate a range of possible binding modes (cf. Scheme 2) and led to the conclusion that positive homotropic allosteric binding behavior[8e,17] was to be expected.[18] The fluoride anion in-binding-modes (*inner*-**3a**·F^-_1, *inner*-**3a**·F^-_2) are more stable by 15.73 and 24.20 kcal/mol, respectively, than alternative species, such as *outer*-

(12) In **3b**·6$CHCl_3$·C_7H_8, four of the six $CHCl_3$ molecules are associated with the nitrogen atoms (N and NH) of the core macrocyclic cavities. Among the four bound $CHCl_3$ molecules, two are coordinated by quinoxaline-N atoms (C−H···N, 3.224 Å), while the others are bound by Schiff-base-N (C−H···N, 3.965 Å) and pyrrolyl-NH (Cl···H−N, 3.596 Å) interactions. On the other hand, analysis of the crystal packing diagrams for **3b**·4$CHCl_3$ and **3c**·6$CHCl_3$ reveal in both cases an association between only two $CHCl_3$ molecules and the hydrogen-bonding sites in the cavities. The two bound $CHCl_3$ molecules in **3b**·4$CHCl_3$ are associated with Schiff-base-N atoms (C−H···N, 3.498 Å), while those in **3c**·6$CHCl_3$ are bound by Schiff-base-N (C−H···N, 3.271 Å) and the neighboring macrocycle-derived pyrrolyl-NH atoms (Cl···H−N, 3.706 Å).

(13) The observed spectral changes presumably reflect differences in the electronic structure of the macrocycle resulting from anion binding. The various effects, including electrostatic and charge transfer phenomena, as well as conformational twisting (i.e., direct orbital overlap) contributions, can lead to the observed spectral changes noted previously[5a] but remains an area of current interest and study.

(14) The binding constants for **3b**−**c** and dihydrogenphosphate proved too low to measure accurately. So, in this report, only **3a** was used for quantitative analyses involving this anion. The low affinities seen for **3b** and **3c** are consistent with the known electron-donating (and anion affinity reducing) ability of alkoxy groups. See: ref 7b.

(15) The proposed 1:2 binding stoichiometry for the anion complexes formed between receptors of type **3** and various small anions was supported by a Job plot made by plotting the changes in the UV−vis absorption spectrum observed as the relative mole fraction of tetrabutylammonium fluoride and **3c** in CH_2Cl_2 were varied (cf. Supporting Information). Solubility considerations precluded carrying out similar studies in the case of systems **3a** and **3b**.

(16) TBAF is not a salt that can be obtained in a completely pure, anhydrous form, and it often contain impurities such as $[F-H-F]^-$ (see: Sharma, R. K.; Fry, J. L. *J. Org. Chem.* **1983**, *48*, 2112−2114). While this lack of purity potentially affects all anion binding analyses involving this species, the relative effects of impurities are likely to be similar for related species, allowing semiquantitative comparisons within generalized receptor classes (e.g., **1a** vs **3a** in the present instance).

Scheme 2. Possible Anion Binding Modes Involving Macrocycle **3a**

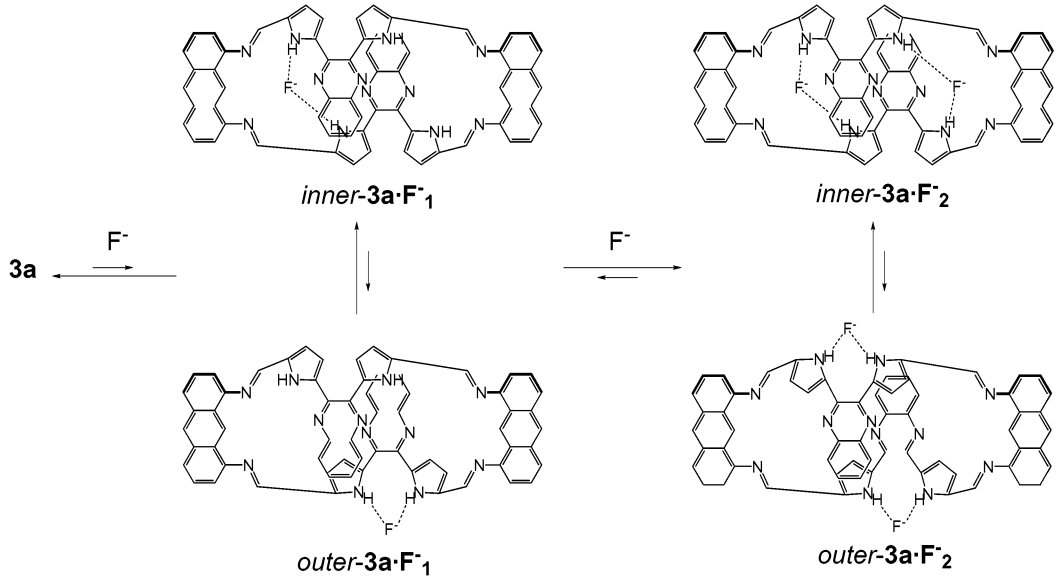

3a·F^-_1 and *outer*-**3a**·F^-_2, wherein the fluoride anion is bound outside the cavity. Further, the distance between the "free" pyrrolic nitrogens in the monoanion complex, *inner*-**3a**·F^-_1 (4.731 Å), is calculated to be 0.117 Å shorter than that observed in the optimized structure of **3a** (4.848 Å). This supports the contention that the binding of the first fluoride anion makes binding the second fluoride anion somewhat more facile. That is, once a fluoride anion is captured in one cavity, the other cavity "shrinks" to the point where its size is better optimized for fluoride anion binding. This is reflected in the fact that the relative energies of (**3a** + $2F^-$) and (*inner*-**3a**·F^-_1 + F^-) are respectively 169.40 and 62.40 kcal/mol greater than that of *inner*-**3a**·F^-_2, the most stable species calculated for this ensemble of species. Although the fluoride anion is actually stabilized to a significant extent by solvents in solution, making free fluoride difficult to obtain in pure form, the effect of such behavior is likely to be energetically equal in the case of the competing "in" and "out" binding modes. Thus, the present theoretical studies support the contention that the quinoxaline-bridged macrocycles (**3**) will display modest positive homotropic allosteric binding when exposed to fluoride and, possibly, other small anions.[18] Such behavior is made possible by the fact that, in contrast to acyclic DPQ derivatives such as **1a**, macrocycles of type **3** contain *two* interconnected NH-rich binding cavities whose inward pointing cores can act as cooperative binding sites.

Figure 4. Color changes induced by the addition of anions (as TBA salts) to solutions of **3a** (2.48×10^{-5} M) in 10% DMSO/CH_2Cl_2 (*v*/*v*). From left to right: **3a**; **3a** + F^- (20 equiv); **3a** + $H_2PO_4^-$ (20 equiv); **3a** + $H_2PO_4^-$ (300 equiv); **3a** + Cl^- (300 equiv).

When taken together, the above findings lead to the conclusion that macrocycle **3a** could be made to function as an improved fluoride and phosphate anion sensor. This point is underscored by Figure 4 that highlights the changes in color induced by the addition of anions to solutions of **3a** in 10% DMSO/CH_2Cl_2 (*v*/*v*).[19] While requiring a greater number of molar equivalents than fluoride, the key point is that $H_2PO_4^-$, like F^-, can deepen the color of **3a**, albeit not that of **1a**,[5a] from pale orange to red. Such changes in color, however, were not observed upon the addition of >300 molar equiv of Cl^-, Br^-, NO_3^-, or HSO_4^- to **3a**. While not established by experiment, this latter finding, which mirrors observations seen in the case of sapphyrins[6] and calix[4]pyrroles,[7] likely mirrors the lower charge density present on these anions relative to those on $H_2PO_4^-$ and F^-. In the case of the oxo-anions, it could also reflect an inability (or, in the case of HSO_4^-, a reduced ability) to engage in X−OH···N_{imine} (X = N, P, or S) hydrogen-bonding interactions, secondary binding effects that could play an ancillary role in stabilizing the dihydrogenphosphate complexes of **3a**.

Conclusion

In summary, we have succeeded in preparing the first macrocycles containing dipyrrolylquinoxaline (DPQ) subunits as bridging elements. As compared to analogous acyclic DPQ

(17) (a) Tylor, P. N.; Anderson, H. L. *J. Am. Chem. Soc.* **1999**, *121*, 11538−11545. (b) Takeuchi, M.; Imada, S.; Shinkai, S. *Angew. Chem., Int. Ed. Engl.* **1998**, *37*, 2096−2099. (c) Ikeda, M.; Tanida, T.; Takeuchi, M.; Shinkai, S. *Org. Lett.* **2000**, *2*, 1803−1805. (d) Sugasaki, A.; Ikeda, M.; Takeuchi, K.; Koumoto, K.; Shinkai, S. *Tetrahedron* **2000**, *56*, 4717−4723. (e) Sugasaki, A.; Ikeda, M.; Takeuchi, M.; Shinkai, S. *Angew. Chem., Int. Ed.* **2000**, *39*, 3839−3842. (f) Ikeda, M.; Shinkai, S.; Osuka, A. **2000**, 1047−1048. (g) Shinkai, S.; Ikeda, M.; Sugasaki, A.; Takeuchi, M. *Acc. Chem. Res.* **2001**, *34*, 494−503. (h) Takeuchi, M.; Ikeda, M.; Sugasaki, A.; Shinkai, S. *Acc. Chem. Res.* **2001**, *34*, 865−873.

(18) Fluoride complexes, which proved easier to optimize that the corresponding dihydrogenphosphate complexes, were used for the bulk of the energy minimization studies. Preliminary optimization of the various putative $H_2PO_4^-$ complexes gave results concordant with those obtained in the case of fluoride. In particular, the "inner" binding mode was found to be more stable than its nearest energy "outer" alternative by ~11.3 kcal/mol for the monoanionic complex. The propensity to bind a second anion in a positive, cooperative manner was also reproduced. As mentioned in the text, analogous UV−vis absorption spectral changes were also seen when binding studies were carried out using these two anions, fluoride and $H_2PO_4^-$ (see also Supporting Information). This provides further support for the contention dihydrogenphosphate is binding in a manner analogous to that of fluoride, with the exception that the phosphate oxo-anion is "sticking in" toward the NH-rich binding site rather than being fully encapsulated. Direct experimental support (solid-state and solution phase) for such a supposition has been previously obtained in the case of sapphyrin.[6b,c]

derivatives, these new systems display augmented anion binding affinities and positive allosteric binding behavior in organic solution, as well as encapsulation of $CHCl_3$ via hydrogen bonding in the solid state. In accord with molecular modeling studies, such enhancements and allosteric effects are thought to reflect the combined effects of preorganization and the presence of two pyrrolic NH donor groups that can act in concert. To the extent such thinking is correct, it leads to the suggestion that other structures containing DPQ "building blocks" could prove useful as receptors, not just for anions but also possibly for neutral and cationic substrates. Efforts to generate such systems are in progress.

Experimental Section

All starting materials were purchased from Aldrich Chemical Co. and used without further purification unless otherwise stated. NMR spectra used in the characterization of products were recorded on a Varian 500 MHz spectrometer. All NMR spectra were referenced to solvent. TLC analyses were carried out using Whatman K6F silica gel 60 Å, 250 mm plates. Column chromatography was performed using Whatman silica gel 60 Å (230−400 mesh). Dipyrrolylquinoxalines **1a**−**c** and 1,8-diaminoanthracene were prepared according to literature procedures.[5a,b,9a]

6,7-Dimethoxy-2,3-bis(pyrrol-2′-yl)quinoxaline, 1b. ^{1}H NMR (500 MHz, $CDCl_3$, rt) δ 9.41 (br, 2H, NH), 7.21 (s, 2H, quinoxaline), 6.94 (m, 2H, pyrrole-H), 6.73 (m, 2H, pyrrole-H), 6.25 (m, 2H, pyrrole-H), 4.01 (s, methoxy, 6H); ^{13}C NMR (125.65 MHz, $CDCl_3$, rt) δ 152.23, 141.67, 136.89, 129.30, 120.13, 111.48, 109.89, 106.19, 56.27. HRMS (CI^+) *m*/*z* ($M + H^+$) calcd for $C_{18}H_{17}N_4O_2$: 321.1348; found, 321.1352. Anal. Calcd for $C_{18}H_{16}N_4O_2$: C, 67.49; H, 5.03; N, 17.49; O, 9.99. Found: C, 67.51; H, 5.08; N, 17.49; O, 9.92.

6,7-Diethoxy-2,3-bis(pyrrol-2′-yl)quinoxaline, 1c. ^{1}H NMR (500 MHz, $CDCl_3$, rt) δ 9.38 (br, 2H, NH), 7.19 (s, 2H, quinoxaline), 6.94 (m, 2H, pyrrole-H), 6.71 (m, 2H, pyrrole-H), 6.25 (m, 2H, pyrrole-H), 4.23 (q, $J = 7.0$ Hz, 4H, CH_2), 1.54 (t, $J = 7.0$ Hz, 6H, CH_3); ^{13}C NMR (125.65 MHz, $CDCl_3$, rt) δ 151.81, 141.52, 136.86, 129.39, 120.01, 111.33, 109.86, 106.95, 64.63, 14.51. HRMS (CI^+) *m*/*z* (M^+) calcd for $C_{20}H_{20}N_4O_2$: 348.1582; found, 348.1586. Anal. Calcd for $C_{20}H_{20}N_4O_2$: C, 68.95; H, 5.79; N, 16.08; O, 9.18. Found: C, 68.84; H, 5.87; N, 15.98; O, 9.31.

2,3-Bis(5′-formylpyrrol-2′-yl)quinoxaline, 2a. $POCl_3$ (240 μL, 2.57 mmol) was added to DMF (454 μL, 5.86 mmol) at 0 °C under Ar. This mixture was then allowed to warm to room temperature and stirred for 10 min before 1,2-dichloroethane (3 mL) was added. To this mixture was then added a solution of the unsubstituted dipyrrolylquinoxaline **1a** (260 mg, 1.00 mmol) in 1,2-dichloroethane (15 mL) over a period of 10 min. The resulting mixture was heated at reflux for 30 min before being cooled to 0 °C. Saturated aqueous NaOAc (3 mL) was then added, and the mixture was heated at reflux for a further 30 min. Upon cooling, the mixture was washed with CH_2Cl_2, and the combined organic phases were then washed with water and brine, dried over anhydrous Na_2SO_4, filtered, and evaporated to dryness. The residue was then subject to chromatography over silica gel (eluent 1% MeOH/CH_2Cl_2) and recrystallized from CH_2Cl_2/hexane to afford **2a** (252 mg, 80%) as a yellow solid: ^{1}H NMR (500 MHz, DMSO-d_6, rt) δ 12.67 (br, 2H, NH), 9.69 (s, 2H, CHO), 8.13 (m, 2H, quinoxaline), 7.90 (m, 2H, quinoxaline), 7.03 (dd, $J = 4.0$ Hz, 2.5 Hz, 2H, βH), 6.15 (dd, $J = 4.0$ Hz, 2.5 Hz, 4H, βH); ^{13}C NMR (125.65 MHz, DMSO-d_6, rt) δ 180.37, 144.35, 140.00, 135.42, 134.05, 130.92, 128.61, 118.81, 112.80. HRMS (CI^+) *m*/*z* ($M + H^+$) calcd for $C_{18}H_{13}N_4O_2$: 317.1039; found, 317.1034. Anal. Calcd for $C_{18}H_{12}N_4O_2$: C, 68.35; H, 3.82; N, 17.71; O 10.12. Found: C, 68.36; H, 3.99; N, 17.78; O, 9.87.

(19) Because of the low solubility of **3a**, it proved necessary to add DMSO in order to obtain solutions suitable for use in the colorimetric studies.

6,7-Dimethoxy-2,3-bis(5′-formylpyrrol-2′-yl)quinoxaline, 2b. $POCl_3$ (280 μL, 3.00 mmol) was added to DMF (530 μL, 6.84 mmol) at 0 °C under Ar. This mixture was then allowed to warm to room temperature and stirred for 10 min before 1,2-dichloroethane (3 mL) was added. To this mixture was then added a solution of the dipyrrolylquinoxaline **1b** (320 mg, 1.00 mmol) in 1,2-dichloroethane (30 mL) over a period of 10 min. The resulting mixture was heated at reflux for 2.5 h before being cooled to 0 °C. Saturated aqueous NaOAc (3 mL) was then added, and the mixture was heated at reflux for a further 1 h. Upon cooling, the mixture was washed with CH_2Cl_2, and the combined organic phases were then washed with water and brine, dried over anhydrous Na_2SO_4, filtered, and evaporated to dryness. The residue was then subject to chromatography over silica gel (eluent 1% MeOH/CH_2Cl_2) and recrystallized from CH_2Cl_2/hexane to afford **2b** (189 mg, 50%) as a yellow solid: ^{1}H NMR (500 MHz, $CDCl_3$, rt) δ 10.24 (br, 2H, NH), 9.62 (s, 2H, CHO), 7.28 (m, 2H, quinoxaline), 6.96 (dd, $J = 4.0$ Hz, 2.5 Hz, 2H, βH), 6.72 (dd, $J = 4.0$ Hz, 2.5 Hz, 4H, βH), 4.07 (s, 6H, methoxy); ^{13}C NMR (125.65 MHz, $CDCl_3$, rt) δ 179.35, 153.99, 139.94, 138.17, 135.55, 133.54, 120.85, 113.17, 106.03, 56.51. HRMS (CI^+) *m*/*z* ($M + H^+$) calcd for $C_{20}H_{17}N_4O_2$: 377.1250; found, 377.1248. Anal. Calcd for $C_{20}H_{16}N_4O_2$: C, 63.82; H, 4.28; N, 14.89; O, 17.00. Found: C, 63.97; H, 4.35; N, 14.99; O, 16.69.

6,7-Diethoxy-2,3-bis(5′-formylpyrrol-2′-yl)quinoxaline, 2c. $POCl_3$ (280 μL, 3.00 mmol) was added to DMF (530 μL, 6.84 mmol) at 0 °C under Ar. This mixture was then allowed to warm to room temperature and stirred for 10 min before 1,2-dichloroethane (3 mL) was added. To this mixture was then added a solution of dipyrrolylquinoxaline **1c** (398.2 mg, 1.14 mmol) in 1,2-dichloroethane (30 mL) over a period of 10 min. The resulting mixture was heated at reflux for 3 h before being cooled to 0 °C. Saturated aqueous NaOAc (3 mL) was then added, and the mixture was heated at reflux for a further 2 h. Upon cooling, the mixture was washed with CH_2Cl_2, and the combined organic phases were then washed with water and brine, dried over anhydrous Na_2SO_4, filtered, and evaporated to dryness. The residue was then subject to chromatography over silica gel (eluent 1% MeOH/CH_2Cl_2) and recrystallized from CH_2Cl_2/hexane to afford **2c** (229 mg, 50%) as a pale yellow solid: ^{1}H NMR (500 MHz, $CDCl_3$, rt) δ 10.24 (br, 2H, NH), 9.61 (s, 2H, CHO), 7.24 (s, 2H, quinoxaline), 6.95 (dd, $J = 4.0$ Hz, 2.5 Hz, 2H, βH), 6.69 (dd, $J = 4.0$ Hz, 2.5 Hz, 4H, βH), 4.27 (q, $J = 7.0$ Hz, 4H, CH_2), 1.57 (t, $J = 7.0$ Hz, 6H, CH_3); ^{13}C NMR (125.65 MHz, $CDCl_3$, rt) δ 179.32, 153.54, 139.72, 138.12, 135.71, 133.48, 120.89, 113.05, 106.58, 64.97, 14.39. HRMS (CI^+) *m*/*z* ($M + H^+$) calcd for $C_{22}H_{21}N_4O_4$: 405.1563; found, 405.1565. Anal. Calcd for $C_{22}H_{20}N_4O_4$: C, 65.34; H, 4.98; N, 13.85; O, 15.82. Found: C, 65.48; H, 5.31; N, 13.22; O, 15.99.

Compound 3a. Concentrated HCl aq (40 μL) was added to a mixture of the diformyl-substituted dipyrrolylquinoxaline **2a** (50.0 mg, 0.158 mmol) and 1,8-diaminoanthracene (35.0 mg, 0.168 mmol) in toluene (75 mL) and methanol (20 mL) solution. The resulting mixture was stirred for 2 h at reflux temperature. After the evaporation and chromatography over silica gel (eluent 3% MeOH/CH_2Cl_2), the orange-colored solid (**3a**, 9.3 mg, 12%) was isolated by recrystallization from CH_2Cl_2/MeOH: ^{1}H NMR (500 MHz, DMSO-d_6, rt) δ 12.27 (br, 4H, NH), 9.49 (s, 2H, anthracene), 8.71 (s, 4H, imine-CH), 8.58 (s, 2H, anthracene), 7.92 (d, $J = 8.5$ Hz, 4H, anthracene), 7.91 (dd, $J = 6.0$ Hz, 3.0 Hz, 4H, quinoxaline), 7.55 (m, 8H, quinoxaline and anthracene), 7.16 (d, $J = 7.0$ Hz, 4H, anthracene), 6.94 (dd, $J = 4.0$ Hz, 2.5 Hz, 4H, βH), 6.36 (dd, $J = 4.0$ Hz, 2.5 Hz, 4H, βH); ^{13}C NMR (125.65 MHz, DMSO-d_6, rt) δ 150.6, 149.4, 143.6, 139.6, 133.4, 132.9, 132.1, 129.7, 128.2, 127.2, 126.3, 125.3, 113.8, 111.2; the other expected peaks could not be observed because of the low solubility of the sample and the resulting poor spectral resolution. HRMS (CI^+) *m*/*z* ($M + H^+$) calcd for $C_{64}H_{41}N_{12}$: 977.3577; found, 977.3588. UV−vis ($CHCl_3$) λ_{max} (nm) 368.5, 431.5.

Compound 3b. Concentrated HCl aq (8 μL) was added to the mixture of the diformyl-substituted dipyrrolylquinoxaline **2b** (12.5 mg,

0.033 mmol) and 1,8-diaminoanthracene (6.9 mg, 0.033 mmol) in toluene (15 mL) and methanol (3 mL) solution, and the mixture was stirred for 3 h at room temperature before 15 μL of triethylamine was added. After the evaporation and column chromatography over silica gel (eluent 0.5% MeOH/CH_2Cl_2), the orange-colored solid (**3b**, 5.1 mg, 28%) was isolated by recrystallization from CH_2Cl_2/MeOH: ^{1}H NMR (500 MHz, $CDCl_3$, rt) δ 10.87 (br, 4H, NH), 10.09 (s, 2H, anthracene), 8.66 (s, 4H, imine-CH), 8.46 (s, 2H, anthracene), 7.92 (d, J = 9.0 Hz, 4H, anthracene), 7.51 (dd, J = 8.5 Hz, 7.0 Hz, 4H, anthracene), 7.25 (d, J = 7.0 Hz, 4H, anthracene), 6.92 (s, 4H, anthracene), 6.61 (d, J = 4.0 Hz, 4H, βH), 6.51 (d, J = 4.0 Hz, 4H, βH), 3.91 (s, 12H, methoxy); ^{13}C NMR (125.65 MHz, $CDCl_3$, rt) δ 152.70, 148.21, 147.35, 138.86, 137.14, 132.95, 132.80, 132.64, 128.52, 126.09, 125.88, 125.56, 120.11, 116.03, 112.87, 110.23, 106.19, 50.83. HRMS (CI^+) m/z ($M + H^+$) calcd for $C_{68}H_{49}N_{12}O_4$: 1097.4000; found, 1097.4004. UV−vis ($CHCl_3$) λ_{max} (nm) ($\epsilon \times 10^{-4}$ (M^{-1} cm^{-1})) 373 (4.5), 447 (5.6). This compound was further characterized by X-ray diffraction analysis.

Compound 3c. Concentrated HCl aq (8 μL) was added to a mixture of the diformyl-substituted dipyrrolylquinoxaline **2c** (39.3 mg, 0.097 mmol) and 1,8-diaminoanthracene (20.4 mg, 0.098 mmol) in toluene (45 mL) and methanol (9 mL) solution, and the mixture was stirred for 3 h at room temperature before 15 μL of triethylamine was added. After the evaporation and silica gel column chromatography (eluent 0.5% MeOH/CH_2Cl_2), the orange-colored solid (**3c**, 2.2 mg, 4%) was isolated by recrystallization from CH_2Cl_2/MeOH: ^{1}H NMR (500 MHz, $CDCl_3$, rt) δ 10.83 (br, 4H, NH), 10.04 (s, 2H, anthracene), 8.62 (s, 4H, imine-CH), 8.46 (s, 2H, anthracene), 7.92 (d, J = 8.5 Hz, 4H, anthracene), 7.51 (dd, J = 8.5 Hz, 7.0 Hz, 4H, anthracene), 7.23 (d, J = 7.0 Hz, 4H, anthracene), 6.92 (s, 4H, anthracene), 6.56 (d, J = 4.0 Hz, 4H, βH), 6.44 (d, J = 4.0 Hz, 4H, βH), 4.12 (q, J = 7.0 Hz, 8H, CH_2), 1.53 (t, J = 7.0 Hz, 12H, CH_3); ^{13}C NMR (125.65 MHz, $CDCl_3$, rt) δ 152.31, 148.40, 147.55, 138.84, 137.22, 133.12, 132.78, 132.48, 128.42, 125.90, 125.46, 120.23, 116.04, 112.73, 110.18, 106.87, 96.13, 64.61, 14.54. HRMS (CI^+) m/z ($M + H^+$) calcd for $C_{72}H_{57}N_{12}O_4$: 1153.4625; found, 1153.4611. UV−vis ($CHCl_3$) λ_{max} (nm) 374.0, 443.5. This compound was further characterized by X-ray diffraction analysis.

Single-Crystal Diffraction Analysis. Data were collected on a Nonius Kappa CCD diffractometer using a graphite monochromator with Mo Kα radiation (λ = 0.71073 Å). Data collection was effected at 153 K using an Oxford Cryostream low-temperature device. Data reduction were performed using DENZO-SMN.[20] The structure was solved by direct methods using SIR92[21] and refined by full-matrix least-squares on F^2 with anisotropic displacement parameters for the non-H atoms using SHELXL-97.[22] The hydrogen atoms were located in a ΔF map and refined with isotropic displacement parameters. $wR(F^2) = \{\Sigma w(|F_o|^2 - |F_c|^2)^2/\Sigma w(|F_o|)^4\}^{1/2}$, where w is the weight given each reflection. $R(F) = \{\Sigma(|F_o| - |F_c|)/\Sigma|F_o|\}$ for reflections with $F_o > 4(\sigma(F_o))$. $GOF = [\Sigma w(|F_o|^2 - |F_c|^2)^2/(n - p)]^{1/2}$, where n is the number of reflections and p is the number of refined parameters. The data were corrected for secondary extinction effects. Neutral atom scattering factors and values used to calculate the linear absorption coefficient are from the International Tables for X-ray Crystallography.[23] Details of the crystal data are listed in Table 1.

Table 1. Crystallographic Details for Compounds **3b** (two structures) and **3c**

	3b·6$CHCl_3$·C_7H_8	**3b**·4$CHCl_3$	**3c**·6$CHCl_3$
emp formula	$C_{81}H_{62}Cl_{18}N_{12}O_4$	$C_{77}H_{52}Cl_{12}N_{12}O_4$	$C_{78}H_{62}Cl_{18}N_{12}O_4$
fw	1905.52	1574.66	1869.50
color, habit	red-orange, prism	orange, lathe	yellow, needle
space group	$P\bar{1}$	$P\bar{1}$	$P\bar{1}$
a, Å	11.8710(1)	11.3486(2)	7.4880(3)
b, Å	14.7773(1)	11.4566(2)	15.8282(6)
c, Å	15.1011(2)	15.2482(3)	18.6874(8)
α, deg	98.764(1)	112.061(1)	103.797(2)
β, deg	113.107(1)	95.776(1)	95.751(2)
γ, deg	113.387(1)	102.885(1)	102.723(2)
V, Å^3	2082.05(4)	1753.39(6)	2086.29(15)
Z	1	1	1
radiation (λ, Å)		Mo Kα (0.710 73)	
T, K	153(2)	153(2)	153(2)
Dc, g/cm^3	1.520	1.491	1.488
μ, mm^{-1}	0.650	0.534	0.647
diffractometer		Nonius Kappa CCD	
R_1	0.0640	0.0797	0.0866
wR_2 (all data)	0.1413	0.137	0.1668
GOF	2.410	1.037	1.606
indep reflns	11 935	7888	9466
obsd reflns ($I > 2\sigma(I)$)	11 935	7888	9466
parameters	514	556	470

Ab Initio Calculation. Ab initio calculations of **3a** and its putative fluoride anion complexes were carried out using the Gaussian 98 program[24] and an HPC-alpha UP264 (HIT) computer. The structures were optimized, and the total electronic energies were calculated at the HF level using a 3-21G basis set.

Acknowledgment. This work was supported by the National Institutes of Health and the R. A. Welch Foundation (Grants GM 58907 and F-1018, respectively, to J.L.S.). H.M. thanks Prof. Atsuhiro Osuka, Graduate School of Science, Kyoto University for a study leave and the JSPS for a Research Fellowship for Young Scientists.

Supporting Information Available: UV−vis titration curves for anion binding studies involving **3a**, Job plots for the association of **3c** and fluoride, Cartesian coordinates of the optimized structures of **3a** and its anion binding complexes, and X-ray structural data for compounds **3b** (two structures) and **3c**. This material is available free of charge via the Internet at http://pubs.acs.org.

JA0273750

(20) Otwinowski, Z.; Minor, W. Macromolecular Crystallography, Part A. Carter, C. W., Jr.; Sweets, R. M., Eds.; *Methods Enzymol.* **1997**, *276*, 307−326.
(21) Altomare, A.; Cascarano, G.; Giacovazzo, C.; Guagliardi, A. *J. Appl. Crystallogr.* **1993**, *26*, 343−350.
(22) Sheldrick, G. M. SHELX-97, Program for the refinement of Crystal Structures; University of Göttingen: Göttingen, Germany, 1994.
(23) *International Tables for X-ray Crystallography*, Vol. C; Kasper, J. S., Lonsdale, K., Eds.; Kluwer Academic Press: Boston, MA; 1992. Tables 4.2.6.8. and 6.1.1.4.
(24) Frisch, M. J.; Trucks, G. W.; Schlegel, H. B.; Scuseria, G. E.; Robb, M. A.; Cheeseman, J. R.; Zakrzewski, V. G.; Montgomery, J. A.; Stratmann, R. E.; Burant, J. C.; Dapprich, S.; Millam, J. M.; Daniels, A. D.; Kudin, K. N.; Strain, M. C.; Farkas, O.; Tomasi, J.; Barone, V.; Cossi, M.; Cammi, R.; Mennucci, B.; Pomelli, C.; Adamo, C.; Clifford, S.; Ochterski, J.; Petersson, G. A.; Ayala, P. Y.; Cui, Q.; Morokuma, K.; Malick, D. K.; Rabuck, A. D.; Raghavachari, K.; Foresman, J. B.; Cioslowski, J.; Ortiz, J. V.; Stefanov, B. B.; Liu, G.; Liashenko, A.; Piskorz, P.; Komaromi, I.; Gomperts, R.; Martin, R. L.; Fox, D. J.; Keith, T.; Al-Laham, M. A.; Peng, C. Y.; Nanayakkara, A.; Gonzalez, C.; Challacombe, M.; Gill, P. M. W.; Johnson, B. G.; Chen, W.; Wong, M. W.; Andres, J. L.; Head-Gordon, M.; Replogle, E. S.; Pople, J. A. Gaussian 98, revision A.9; Gaussian, Inc.: Pittsburgh, PA, 1998.